

**Homogenization of plastic deformation in metallic glass foils less than one micrometer thick**A. R. Yavari,<sup>1,2,3,4</sup> K. Georgarakis,<sup>2,1</sup> W. J. Botta,<sup>3,1</sup> A. Inoue,<sup>2</sup> and G. Vaughan<sup>4</sup><sup>1</sup>*Institut Polytechnique de Grenoble (INPG), Euronano SIMaP-CNRS, 38402, St-Martin-d'Herès Campus, France*<sup>2</sup>*WPI AIMR, Tohoku University, Sendai 980-8577, Japan*<sup>3</sup>*Department of Materials Engineering (DeMa), Federal University of São Carlos (UFSCar), CEP 13565-905, São Carlos, São Paulo, Brazil*<sup>4</sup>*European Synchrotron Radiation Facility (ESRF), Grenoble, France*

(Received 19 September 2010; published 9 November 2010)

Metallic glasses do not possess crystalline structures with slip systems that provide for plastic deformation via dislocation glide. As such, when put under applied stress, they show a wide reversible elastic deformation  $\epsilon_{el} \approx 2\%$  before plastic flow occurs heterogeneously by localization in shear bands only tens of nanometers in thickness. Very recently, there have been reports that in microscopic (submicron thickness) pillars, such shear bands no longer form and deformation occurs homogeneously. Here we report on plastic deformation of submicron thickness foils of metallic glasses. When such foils are compressed or notched, a similar transition occurs from the usual heterogeneous plastic deformation mode via shear banding to more homogeneous deformation without formation of shear bands. Some shape instabilities in the form of vortices observed at interfaces between plastic zones and nondeformed regions are consistent with sharp deformation-induced density, velocity, and viscosity gradients. The onset of homogeneous deformation in the microscopic regime is discussed in relation to shear-band formation energy and thickness.

DOI: [10.1103/PhysRevB.82.172202](https://doi.org/10.1103/PhysRevB.82.172202)

PACS number(s): 81.05.Kf, 61.43.Dq, 62.20.fq, 81.40.Lm

Unlike crystalline metals, metallic glasses do not have a periodic lattice with glide planes on which mobile dislocation can cause plastic flow. Consequently, they show a wide elastic strain range on the order of 2% before the onset of plastic deformation which occurs in a highly localized manner on planes of maximum shear stress at approximately 45° to the applied load axis.<sup>1-3</sup>

Plastic deformation results in the generation of free volume and local heating which, in turn, lower local viscosity leading to shear softening that contributes to further localization of deformation in narrow shear bands 1–20 nm in thickness.<sup>4-7</sup> Because of the heterogeneous nature of this type of deformation, only matter in the shear bands undergoes plastic deformation with plastic strains on the order of 1–1000 usually leading to fracture.

A contrary behavior was recently reported for some microscopic metallic glasses. Guo *et al.*<sup>8</sup> reported significant tensile ductility via homogeneous deformation followed by necking in 100 nm thick and about 600 nm pillars carved by a focused ion beam (FIB) within a plate-shaped metallic glass. However, some attributed their observed homogeneous deformation to the nonfree-standing nature of the pillars.

Homogeneous deformation in compression of FIB-machined submicron pillars (for example, 400 nm diameter and 1  $\mu\text{m}$  length) was reported by Volkert *et al.*<sup>9</sup> and by others<sup>10</sup> while some have reported only heterogeneous deformation down to the lowest specimen dimensions.<sup>11,12</sup> More recent work by Jang and Greer<sup>13</sup> confirmed extensive tensile ductility via homogeneous deformation at low strain rates in free-standing submicron (100 nm thickness and 1  $\mu\text{m}$  length) metallic glass pillars. The latter work was also significant in that any room-temperature plasticity in tensile tests of free-standing metallic glasses had only been observable at very high strain rates.<sup>14-16</sup>

Homogeneous deformation and significant ductility of microscopic metallic glasses both in tension and compression

removes the historically established limiting tradeoff between materials strength and ductility. In fact, some reports indicate that the ductile behavior in this size range is accompanied by significant increase in mechanical strength as compared to bulk metallic glasses.<sup>13</sup> But these phenomena are as yet not well understood.

Lacking the usual dislocation glide planes for plastic deformation, metallic glasses store a large amount of elastic energy (resilience)  $E_{el}$  prior to the onset of plastic deformation after reaching elastic strain  $\epsilon_{el} \geq 2\%$  at applied stress  $\sigma = E\epsilon_{el}$ , where  $E$  is Young modulus (Hook's law). In their report of such homogeneous deformation, Volkert *et al.*<sup>9</sup> postulated that if this stored elastic energy  $E_{el} = V(1/2)\sigma\epsilon_{el} = V(1/2)E\epsilon_{el}^2$  which scales with the specimen volume  $V$  is less than that required to create a shear band across the specimen cross section, plastic deformation can only occur homogeneously. Stored elastic energy scales with sample volume while the shear-band creation energy  $E_{sb}$  scales with the sample cross section. For a glassy cylindrical pillar of height  $h$  and diameter  $d = 2r$ ,  $V = \pi r^2 h$  and the stored elastic energy at the onset of plastic deformation is

$$E_{el} = \pi r^2 h (1/2) \sigma \epsilon_{el} = (1/2) \pi (d/2)^2 h E \epsilon_{el}^2 \quad (1)$$

while the shear-band formation energy would be

$$E_{sb} = 2^{1/2} \pi (d/2)^2 \Gamma_{sb}, \quad (2)$$

where  $\Gamma_{sb}$  stands for shear-band energy per unit area and the factor  $2^{1/2}$  is due to the approximately  $\pi/4$  angle of the band to the applied load direction.

Setting these two energy terms equal as in Ref. 9, a critical height  $h_{crit}$  is obtained below which there is not enough stored mechanical energy available for the creation of a shear band

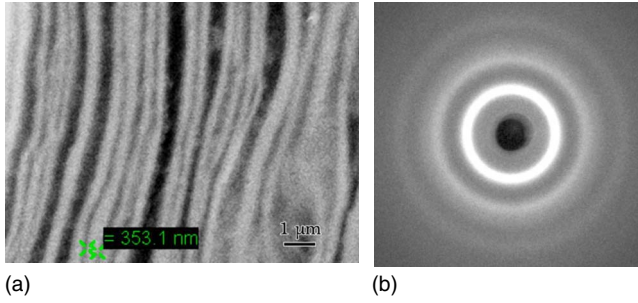


FIG. 1. (Color online) (a) Stack of foils of  $Zr_{57}Cu_{14.4}Ni_{12.6}Al_{10}Nb_5$  metallic glass obtained by mechanical deformation of melt-spun ribbons and (b) its x-ray diffraction pattern in transmission.

$$h_{\text{crit}} = 2^{3/2} \Gamma_{\text{sb}} / E \varepsilon_{\text{el}}^2. \quad (3)$$

It is notable that Eq. (3) predicts end of the heterogeneous regime of deformation as  $h$ , the specimen height in the direction of the applied load is lowered to  $h_{\text{crit}}$  and is independent of the aspect ratio of the metallic glass. In Ref. 9, the pillar had an aspect ratio  $\alpha = h/d = 2.5$  and the critical height corresponded to the critical diameter

$$d_{\text{crit}} = 2^{3/2} \Gamma_{\text{sb}} / \alpha E \varepsilon_{\text{el}}^2. \quad (4)$$

Below  $d_{\text{crit}}$  the available elastic energy would not be enough to form a shear band across the pillar cross section.

In the tensile experiment of Jang and Greer,<sup>13</sup> the metallic glass rod had an effective aspect ratio (after correction for tapering) of  $\alpha \leq 8$  with  $h \leq 1 \mu\text{m}$  and  $d \approx 100 \text{ nm}$ . Following Volkert *et al.*,<sup>9</sup> they defined their “critical size” for the transition from the heterogeneous to homogeneous deformation regime in terms of a “critical diameter.”

The independence of Eq. (3) from the aspect ratio raises the interesting question as to the existence of a homogeneous deformation regime for submicron-thick foils of metallic glasses when mechanically solicited along the thin direction, which is the subject of this report.

$Zr_{57}Cu_{14.4}Ni_{12.6}Al_{10}Nb_5$  metallic glass was produced in the form of  $\sim 30\text{-}\mu\text{m}$ -thick ribbons by melt spinning on a rotating copper wheel under argon atmosphere. Their thickness was then progressively “hammered” down to submicron-thick foils by deformation between a large vertically vibrating steel ball and an anvil.<sup>17</sup> The thin deformed foils were examined by x-ray diffraction in transmission as well as electron microscopy using a LEO S440 scanning electron microscope (SEM) and a FEI/Philips Technai F20 transmission electron microscope (TEM).

It has previously been reported that deformation of metallic glasses leads to some nanocrystallization in or near shear bands.<sup>18–20</sup> Figure 1(b) shows an x-ray diffraction image obtained using a monochromatized synchrotron light in transmission through a stack of foils deformed to submicron thicknesses [Fig. 1(a)] and no trace of crystallinity can be detected. Numerous electron-diffraction patterns obtained by TEM also failed to reveal presence of any crystallinity in the thin foils.

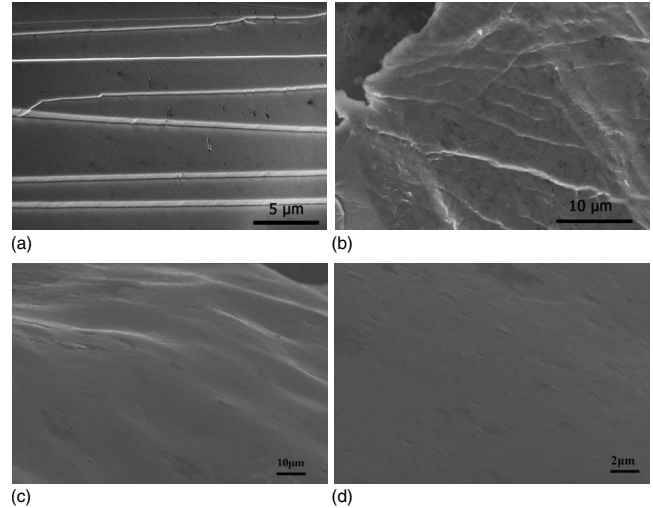


FIG. 2. (a) SEM images of shear steps on the surface of the Zr-based metallic glass melt-spun ribbon after bending and same ribbon after heavily deformation reduced thickness to about (b)  $2 \mu\text{m}$  and [(c) and (d)] less than  $500 \text{ nm}$ .

The operation of shear bands results in the appearance of shear steps (or offsets) on the specimen surface which can be observed by optical, scanning electron, or atomic force microscopy. Figure 2 shows SEM image of shear steps on the surface [Fig. 2(a)] of the melt-spun Zr-based metallic glass ribbon after bending and [Fig. 2(b)] a foil made from same ribbon after heavy deformation reduced its thickness to about  $2 \mu\text{m}$ . Shear steps can be easily observed on the deformed foil surface, clearly indicating that deformation occurred by heterogeneous plastic flow localized in shear bands that generate visible steps  $100 \mu\text{m}$  long on the foil surface. Step heights seem to vary on the order of  $1 \mu\text{m}$  or less.

Continued deformation as applied to foil of Fig. 2(b) reduced thicknesses down to submicron scale and as low as  $250\text{--}300 \text{ nm}$  and Figs. 2(c) and 2(d) show SEM images of the surface of such a foil. To the resolution of these images, shear steps that are the fingerprint of shear bands [Fig. 2(b)] have disappeared from the surfaces of these thinner glassy foils indicating that at or near these thicknesses, the plastic deformation that reduces foil thickness occurs rather homogeneously.

While observation of shear steps down to tens of nanometers on the surfaces of metallic glasses is straight forward using SEM, tracing shear bands using TEM is more challenging. Shear bands mostly appear as more clear regions. This contrast may be due to less number of atoms per unit area (lower thickness) or higher deformation-induced free-volume content either distributed homogeneously or precipitated to form nanoscale pores.<sup>4,21</sup> Figure 3 shows TEM images of glassy foils deformed down to thicknesses around  $800 \text{ nm}$  [Fig. 3(a)] and  $300 \text{ nm}$  [Fig. 3(b)], respectively, and then ion milled for TEM transparency. The presence of contrast zones likely due to shear bands can be seen near the ion-milled hole in the thicker foil as indicated. Shear-band thickness is generally expected to be  $10\text{--}20 \text{ nm}$  (Refs. 4 and 5) but these bands are at  $45^\circ$  angle to the foil plane and thus appear thicker. On the other hand, no such contrast areas

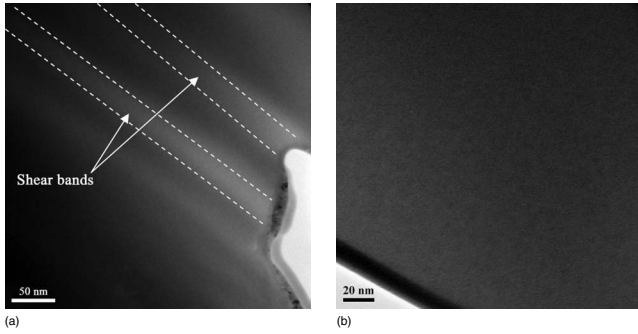


FIG. 3. TEM images of glassy foils heavily deformed down to thickness around (a) 800 nm and (b) 300 nm.

were detected in the foil deformed down to thickness around 300 nm.

These observations indicate that when very thin glassy foils are mechanically solicited in the thickness direction, deformation occurs by what appears to be a homogenous mechanism in agreement with the recently reported size-induced transition for pillars and rods.<sup>9,13</sup>

The above disappearance of traces of thin shear bands after heavy deformation of thin foils can be compared to plastic deformation of thin films prepared from macroscopic metallic glass specimens for TEM observations. Depending on the specimen absorption coefficients, TEM transparent regions of such films are usually well below 100 nm thick near holes that result from ion milling or electropolishing. Donovan and Stobbs<sup>21</sup> extensive TEM investigation of shear bands in metallic glasses included an image of a crack that accidentally propagated from a hole inward and a zone with bright contrast appeared around and ahead of the crack. We have observed plastic zones of bright contrast in TEM transparent zones of *in situ* deformed foils of metallic glasses.<sup>22,23</sup>

Figures 4(a) and 4(b) show the plastic zone with bright contrast in front of a crack propagating *in situ* from the ion-milled hole into a Zr-based metallic glass thinned to TEM transparency. The width of the plastic zone is about 200 nm, far wider than the thickness  $d_{sb} \approx 10$  nm of a shear band implying that the deformation is more homogeneous and less localized in such thin specimens. The bright plastic zone is seen to advance nearly 1  $\mu\text{m}$  ahead of the crack where it fades as the specimen becomes too thick. The argument could be advanced that these wide bright contrast zones are, in fact, very thin (10–20 nm) shear bands running at an angle to the plane of the film and such a band at  $\pi/4$  angle to the incident beam would indeed have a projected width equal to the film thickness most likely increasing from tens of nanometers to some 200 nm away from the crack where the film has near zero transparency. However, following Donovan and Stobbs,<sup>21</sup> to observe this type of broad contrast in TEM, the contrast zones must be at least some 10% less dense (contain voids or be thinner). If they constitute, as it would be the case for a 10-nm-thick shear band within a film of, say, 100 nm thickness, then the overall electron-density reduction would be 1% and would go undetected. The bright contrast zones ahead of the crack are therefore not thin shear bands but wide plastic zones with width equal or superior to the film thickness.

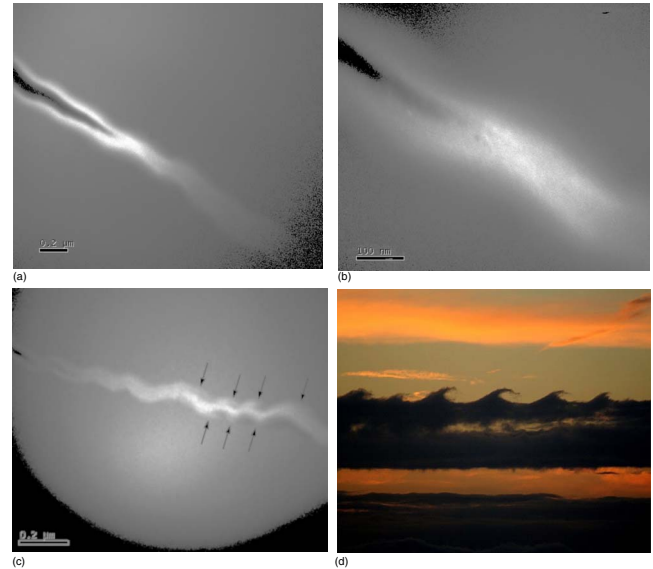


FIG. 4. (Color online) [(a) and (b)] Plastic zone with bright contrast in front of a crack propagating *in situ* from the ion-milled hole in Zr-based metallic glass. The width of the plastic zone is about 200 nm. (c) Wavy plastic zone ahead of a crack in a Cu-Zr metallic glass with tendency to form vortex-shape instabilities (see arrows). (d) Similarly shaped billow cloud (Ref. 26) on a scale  $10^9$  times that of (c).

Figure 4(c) is the image of the plastic zone running up to 1  $\mu\text{m}$  ahead of a crack in an *in situ* deformed Cu-Zr metallic glass containing a small volume fraction of 2 nm size crystallites.<sup>22</sup> Again the width of the bright contrast zone is much wider than that expected for deformation localized into 10–20-nm-thick shear bands. Interestingly, the plastic zone is wavy with tendency to form vortex shapes (see black arrows) as observed in shear-induced hydrodynamic instabilities in fluids,<sup>24</sup> atmospheric and cosmic events due to the Kelvin-Helmholtz (K-H) instability.<sup>25</sup> For comparison, a case of such instability in a “billow cloud” over San Francisco is shown in Fig. 4(d).<sup>26</sup> The shapes are quite similar in the images in Figs. 4(c) and 4(d) but the scales are different by nine orders of magnitude. In metals, K-H flow instability occurs in deformation zones under sharp viscosity, density, and temperature gradients conditions and has, for example, been reported in adiabatic shearing of steels<sup>27</sup> and in high-pressure torsion of other metals.<sup>28</sup> Its appearance in plastic zones ahead of cracks in metallic glass thin films is consistent with sharp viscosity drop expected with severe plastic deformation and the accompanying density and velocity gradients at the borders of the plastic zones where low Richardson numbers are expected.

Going back to the critical dimensions for the glass to attain the microscopic homogeneous plastic deformation regime, Volkert *et al.*<sup>9</sup> considered the energy needed to create a shear band  $\Gamma_{sb}$  to correspond to the mechanical energy per unit volume  $\sigma\epsilon$  for deforming matter within a shear band to a strain of  $\epsilon \approx 1$ , considering that further deformation would not create significantly further disorder. Since the yield stress  $\sigma$  ranges from about 1 GPa for the soft Al-based to over 5 GPa for Co-based metallic glasses,<sup>29</sup> in terms of energy,  $\sigma\epsilon$

corresponds  $10^4$  to  $5 \times 10^4$  J/mole and is superior to  $-\Delta H_{\text{fusion}}$ , the enthalpy of fusion. In fact shear-band melting has been reported in macroscopic specimens of metallic glasses.<sup>6,7</sup> For a shear-band thickness of  $d_{\text{sb}}=10$  nm, this approach gives  $\Gamma_{\text{sb}} \approx 10^{-8} \sigma = 10^{-8} E \epsilon_{\text{el}}$  in units of joule per square meter. Substitution of this expression for  $\Gamma_{\text{sb}}$  in Eq. (3) yields  $h_{\text{crit}} \approx 1400$  nm using  $\epsilon_{\text{el}} \approx 2\%$  for metallic glasses which is just above the length of specimens Volkert *et al.*<sup>9</sup> and Jang and Greer<sup>13</sup> along the load axis. Instead of  $\Gamma_{\text{sb}} \approx 10^{-8} E \epsilon_{\text{el}}$ , if we use  $\Gamma_{\text{sb}} \approx 10^{-8} \mu \gamma_{\text{el}}$ , where shear modulus  $\mu = E/2(1 + \nu)$ , Poisson ratio  $\nu \approx 0.35$  and the universal shear elastic limit  $\gamma_{\text{el}} \approx 2.67\%$ ,<sup>30</sup> Eq. (3) yields  $h_{\text{crit}} \approx 690$  nm which is just below the thickness of the thinnest deformed foil in which we observed shear bands.

It is interesting to note that in this approximation, the critical metallic glass sample dimension for the onset of homogeneous deformation is independent of mechanical strength and chemical composition. This is a consequence of approximating the shear-band energy per unit area  $E_{\text{sb}} \approx d_{\text{sb}} E \epsilon_{\text{el}}$  using the same shear-band thickness  $d_{\text{sb}}$  for all metallic glasses.

Thickness  $d_{\text{sb}}=10$  nm and energy  $\Gamma_{\text{sb}} \approx 10\text{--}50$  J/m<sup>2</sup> can also be compared to typical boundary thicknesses  $d_{\text{gb}} \leq 1$  nm depending on their crystalline structure,<sup>31</sup> grain boundary energies  $\Gamma_{\text{gb}} \approx 0.3\text{--}1$  J/m<sup>2</sup> for various metals.<sup>32</sup> The Volkert approach is thus likely to provide an upper bound value for  $\Gamma_{\text{sb}}$  leading to an upper bound value for the critical sample size  $h_{\text{crit}}$ . Depending on the composition, a lower value of  $\Gamma_{\text{sb}}$  and  $h_{\text{crit}}$  would imply further restriction of the onset of homogeneous mode of room-temperature plastic flow in microscopic metallic glasses and this may in part

explain its nonobservance for some chemical compositions.<sup>11,12</sup>

If the deformation of granular materials are used in qualitative analogy to that of a metallic glass, we may note that shear-band thicknesses in the former are a multiple of grain size as a critical minimum number of grains are required to participate in load transfer toward surfaces and internal defects in order for the dilatation that is required for shear-band formation to occur.<sup>33</sup>

The atomic structure of metallic glasses is not a random packing of grains or atoms. It is rather a close packing of efficiently packed clusters of atoms with shapes, chemistries and dimensions (just under 1 nm) that depend on the alloy composition.<sup>34–37</sup> These atom clusters define the topological and chemical short-range atomic order (CSRO) and their connectivity the medium-range order (MRO). The shear-band thickness  $d_{\text{sb}}$  and energy  $\Gamma_{\text{sb}}$  in metallic glasses are therefore likely to vary with the composition, the atomic CSRO and MRO and thermomechanical history.

In conclusion, it is found that when foils of metallic glasses are compressed or cracked, a transition occurs from the usual heterogeneous plastic deformation mode via shear banding to more homogeneous deformation without formation of shear bands at submicron thicknesses. Shape instabilities in the form of vortices at interface between plastic zones and nondeformed regions are consistent with sharp deformation-induced density, velocity, and viscosity gradients.

This work was supported in part by the EU Marie Curie Network contract ‘‘Ductile BMG Composites.’’ Thanks are due to A. J. Moreira Jorge of DeMa for precious advice concerning the TEM observations.

<sup>1</sup>R. D. Conner *et al.*, *J. Appl. Phys.* **94**, 904 (2003).

<sup>2</sup>Z. F. Zhang *et al.*, *Acta Mater.* **51**, 1167 (2003).

<sup>3</sup>A. R. Yavari *et al.*, *MRS Bull.* **32**, 635 (2007).

<sup>4</sup>J. Li *et al.*, *Philos. Mag. A* **82**, 2623 (2002).

<sup>5</sup>Y. Zhang and A. L. Greer, *Appl. Phys. Lett.* **89**, 071907 (2006).

<sup>6</sup>J. J. Lewandowski and A. L. Greer, *Nature Mater.* **5**, 15 (2006).

<sup>7</sup>K. Georgarakis *et al.*, *Appl. Phys. Lett.* **93**, 031907 (2008).

<sup>8</sup>H. Guo *et al.*, *Nature Mater.* **6**, 735 (2007).

<sup>9</sup>C. A. Volkert *et al.*, *J. Appl. Phys.* **103**, 083539 (2008).

<sup>10</sup>X. L. Wu *et al.*, *Acta Mater.* **57**, 3562 (2009).

<sup>11</sup>B. E. Schuster *et al.*, *Acta Mater.* **56**, 5091 (2008).

<sup>12</sup>A. Dubach *et al.*, *Scr. Mater.* **60**, 567 (2009).

<sup>13</sup>D. C. Jang and J. R. Greer, *Nature Mater.* **9**, 215 (2010).

<sup>14</sup>A. V. Sergueeva *et al.*, *Scr. Mater.* **50**, 1303 (2004).

<sup>15</sup>K. Hajlaoui *et al.*, *Rev. Adv. Mater. Sci.* **18**, 23 (2008).

<sup>16</sup>Y. Yokoyama *et al.*, *Philos. Mag. Lett.* **89**, 322 (2009).

<sup>17</sup>A. R. Yavari *et al.*, *Acta Mater.* **53**, 1611 (2005).

<sup>18</sup>K. Hajlaoui *et al.*, *J. Non-Cryst. Solids* **353**, 327 (2007).

<sup>19</sup>T. Zhang and H. Men, *J. Alloys Compd.* **10**, 434 (2007).

<sup>20</sup>J.-J. Kim *et al.*, *Science* **295**, 654 (2002).

<sup>21</sup>P. E. Donovan and W. M. Stobbs, *Acta Metall.* **29**, 1419 (1981).

<sup>22</sup>K. Hajlaoui *et al.*, *Scr. Mater.* **54**, 1829 (2006).

<sup>23</sup>D. V. Louzguine-Luzgin *et al.*, *Philos. Mag. Lett.* **90**, 139 (2010).

<sup>24</sup>H. J. S. Fernando, *Annu. Rev. Fluid Mech.* **23**, 455 (1991).

<sup>25</sup>W. J. Kelvin, *Philos. Mag.* **42**, 62 (1871).

<sup>26</sup>[http://commons.wikimedia.org/wiki/File:Kelvin\\_Helmholz\\_wave\\_clouds.jpg](http://commons.wikimedia.org/wiki/File:Kelvin_Helmholz_wave_clouds.jpg)

<sup>27</sup>P. R. Guduru *et al.*, *Phys. Rev. E* **64**, 036128 (2001).

<sup>28</sup>Y. Cao *et al.*, *J. Mater. Sci.* **45**, 4545 (2010).

<sup>29</sup>A. Inoue *et al.*, *Nature Mater.* **2**, 661 (2003).

<sup>30</sup>W. L. Johnson and K. Samwer, *Phys. Rev. Lett.* **95**, 195501 (2005).

<sup>31</sup>R. W. Cahn and P. Haasen, *Physical Metallurgy*, 4th ed. (North-Holland, Amsterdam, 1996), Vol. 1, p. 852.

<sup>32</sup>D. Negri *et al.*, *Acta Mater.* **47**, 4545 (1999).

<sup>33</sup>B. Francois *et al.*, *Phys. Rev. E* **65**, 031311 (2002).

<sup>34</sup>D. B. Miracle, *Nature Mater.* **3**, 697 (2004).

<sup>35</sup>H. W. Sheng *et al.*, *Nature (London)* **419**, 439 (2006).

<sup>36</sup>A. R. Yavari, *Nature Mater.* **4**, 2 (2005).

<sup>37</sup>A. R. Yavari, *Nature (London)* **439**, 405 (2006).